Journal Pre-proof

Evaluation of low-cost geo-adsorbents for As(V) removal

Natalia Inchaurrondo, Carla di Luca, Patricia Haure, Gregor Žerjav, Albin Pintar, Cristina Palet

PII: S2352-1864(20)31641-2
DOI: https://doi.org/10.1016/j.eti.2020.101341
Reference: ETI 101341

To appear in: *Environmental Technology & Innovation*

Received date : 7 October 2020
Revised date : 14 December 2020
Accepted date : 22 December 2020

Please cite this article as: N. Inchaurrondo, C. di Luca, P. Haure et al., Evaluation of low-cost geo-adsorbents for As(V) removal. *Environmental Technology & Innovation* (2020), doi: https://doi.org/10.1016/j.eti.2020.101341.

Evaluation of low-cost geo-adsorbents for As(V) removal

Natalia Inchaurrondo[1,*], Carla di Luca[1], Patricia Haure[1], Gregor Žerjav[2], Albin Pintar[2], Cristina Palet[3]

[1]*Department of Chemical Engineering, Institute of Materials Science and Technology (INTEMA), University of Mar del Plata and National Research Council (CONICET), Av. J. B. Justo 4302, 7600 Mar del Plata, Argentina*

[2]*Laboratory for Environmental Sciences and Engineering, Department of Inorganic Chemistry and Technology, National Institute of Chemistry, Hajdrihova 19, SI-1001 Ljubljana, Slovenia*

[3]*Centre Grup de Tècniques de Separació en Química, Department of Chemistry, Universitat Autònoma de Barcelona, 08193 Barcelona, Catalunya, Spain*

Abstract – Four low-cost iron-bearing geo-adsorbents were tested for As(V) removal without pretreatment: Montanit300® (M), diatomite (D), pumice (P) and black sand (BS). The solids were carefully characterized by different analytical techniques (SEM-EDX, TPD-pyridine, N_2 Physisorption, XRD and point of zero charge). The adsorption of As(V) was evaluated through isotherms and kinetic studies (bottled water matrix, pH_0=8, 25 g/L of solids), and experiments addressing pH effect (pH_0=3.6, 7.5, 11) and the presence of interfering anions (Cl^-, SO_4^{2-}, NO_3^-, PO_4^{3-}). Experimental results were fitted to the Freundlich and Langmuir sorption isotherms. Under the employed conditions, P showed negligible adsorption, M and D presented adsorption capacities around 0.02 mg/g and, in spite its lower surface area, BS displayed the highest value (0.045 mg/g),

*Corresponding author. *E-mail address:* ninchaurrondo@gmail.com.

which relates to a higher density of Fe species. M and D samples were easily regenerated (80-100 % desorption) through a basic treatment (0.01 M NaOH) and presented fast adsorption kinetics (1 h for D and seconds for M). BS showed a slow adsorption kinetic (24 h) and poor regeneration (only 50% desorption). Sample M (natural zeolite) resulted a promising option due to its remarkably fast adsorption kinetic, easy regeneration and adsorption capacity suitable for systems with relatively low As concentrations.

Keywords: geo-adsorbents, As(V) removal, adsorption mechanism, Fe-bearing minerals

1. Introduction

The occurrence of arsenic in underground and surface water resources is of great concern since it represents a high risk for human health. Arsenic has been linked to skin and vascular diseases, liver, bladder, lung, kidney and prostate cancer (Palma-Lara et al. 2020). Hence, the World Health Organization has suggested a limit of 10 ppb for drinking water (WHO, 2011). The presence of As in the environment is commonly triggered by biological activity, geochemical and weathering reactions, volcanic emissions and anthropogenic activities such as petroleum refineries, mining/smelting operations, manufacture of certain ceramics or glass, and the use of pesticides and fertilizers (Litter et al. 2010). In Argentina, the presence of arsenic in water is a serious problem which centers the attention of many research groups, focusing their studies on arsenic distribution in different areas of the country and water remediation (Litter et al. 2010).

The removal of arsenic in large scale is usually achieved by coagulation/precipitation reactions using Fe or Al salts, generating a great amount of sludge as unwanted waste**. Therefore, the implementation of cleaner processes such as membrane filtration,**

bioremediation or adsorption technologies has been impelled. Among them, the adsorption process results a very promising alternative owing to its easy operation; reduced cost; no chemical requirement; no sludge generation; low energy consumption and regeneration capability (Burakov et al. 2018). Based on these features, a wide diversity of materials have been studied as adsorbents for the removal of organic and inorganic pollutants: granular activated carbon (GAC) (Kalaruban et al. 2019); activated alumina (Ghosh and Gupta 2012); waste carbonaceous materials (Singh et al. 2020); polymeric adsorbents (Wei et al. 2018; Liu et al. 2020); magnetite nanoparticles (Gu et al. 2018; Wang et al. 2018); iron oxide based sorbents (Siddiqui and Chaudhry 2017); bio-adsorbents and biochar (Gupta et al. 2015; Suhas et al. 2016; Zhao et al. 2020). In particular, the adsorption technology is highly appropriate when sophisticated and expensive techniques cannot be applied, which is the situation of populations with low economical resources. Accordingly, several strategies have emerged, such as the preparation of adsorbents from waste materials (Gupta et al. 2015, 2016; Ahmaruzzaman and Gupta 2011) or the use of cost-effective naturally-occurring adsorbent materials (Asere et al. 2019), which is the topic of the present study.

Several authors investigated the use of soils (Maji et al. 2007; Boglione et al. 2019), diatomites (Danil de Namor et al. 2012), sand (Bajpai and Chaudhuri 1999; Thirunavukkarasu et al. 2003), clays (Manning 1996; Zehhaf et al. 2015), and zeolites (Elizalde-González et al. 2001) in adsorption processes. However, most studies focused on the modification of these natural adsorbents through diverse techniques (impregnation, acid/base treatments) and the usage of the raw materials has not been studied in equal depth.

Oxides and hydroxides of iron, aluminum and manganese, which have shown high affinity towards As, exist ubiquitously in natural environments. **Therefore, the use of these raw materials without preliminary modifications is an interesting and practical option**

that could decrease the cost of the adsorption process and ease its implementation. The element which best associates with As in geo-adsorbents is Fe, due to its high abundance and strong binding affinity (Siddiqui and Chaudhry 2017; Smedley and Kinniburgh 2002). Accordingly, this study focuses on the screening and comparison of four natural Fe-bearing materials of different characteristics: pumice, diatomite, black sand, and Montanit300®, for As(V) removal. These materials have been previously tested as catalysts in the Fenton-Like reaction, showing promising results regarding the mineralization of organic pollutants (Inchaurrondo et al. 2018).

Diatomite is a sedimentary rock composed of microfossils of aquatic algae. It **contains** a large quantity of silica in its structure and the acid sites **present** on its surface are associated to clay impurities with a high content of Al or Fe, **elements** which have shown high affinity towards As in adsorption processes (Danil de Namor et al. 2012). Several studies have reported the use of diatomite for arsenic removal, but generally modified by iron and/or manganese addition (Danil de Namor et al. 2012). In this work, we propose to study the raw material, since the Fe present in its structure proved to be available and active for the catalytic oxidation of organic compounds (Inchaurrondo et al. 2018).

Pumice is a porous volcanic rock with an elevated silica content, which has been tested for the adsorption of different organic and inorganic pollutants (Çifçi and Meriç 2016), typically as a support material or modified through different techniques. In comparison to other studied samples (Çifçi and Meriç 2016), the pumice chosen in this work presents a rather high content of Al and Fe species **(Inchaurrondo et al. 2018).**

Natural aluminosilicate Montanit300® (Montana Žalec, Slovenia) is mostly composed of quartz and natural zeolites like clinoptilolite and heulandite. Some authors studied the application of synthetized or modified zeolites for As removal, frequently through the addition of iron (Bilici Baskan and Pala 2011; Shevade and Ford 2004; Šiljeg et al. 2012). As

mentioned before, the use of the raw material has not been studied in equal depth. Natural zeolites have shown a good ion-exchange capacity for cations, releasing non-toxic ions (K^+, Na^+, Ca^{2+} and Mg^{2+}) to the environment. In the case of anions, the retention in zeolites cavities has been connected to strong interactions with extra-framework cations and Brønsted acid sites (Uzunova and Mikosch 2016).

The black sand used in this study was collected in Praia Preta, Ilha Grande (Brazil) and it is essentially composed of ilmenite, hematite and quartz (**Inchaurrondo et al. 2018**). **It has been reported the use of quartz sand (inert support), modified through the addition of iron, for arsenic removal at laboratory or higher scale (Thirunavukkarasu et al. 2003). In contrast** to the quartz sand frequently studied, a composition rich in Fe species characterizes the sample chosen in this work, which is expected to promote As removal.

The novelty of this work lies in the comparison of cost-effective geo-adsorbents, all widely available, but with different surface structure and composition, in order to select the most efficient material based on adsorption capacity, kinetics and regeneration capability. All natural materials were used in their raw condition without any further expensive treatment. The comparison of the materials was performed taking into consideration that the adsorption process depends on the surface characteristics (specific surface area, surface acidity and point of zero charge) and composition of the adsorbents, the water pH and the presence of interfering ions.

2. Experimental

2.1. Materials

$Na_2HAsO_4 \cdot 7H_2O$ (Aldrich), NaOH, HNO_3 (70% wt/wt, Cicarelli), NaCl (100%, WWR Chemicals), $NaNO_3$ (99%, Aldrich), Na_2SO_4 (99%, Panreac), $Na_2HPO_4 \cdot 7H_2O$ (Aldrich),

$CH_3COONa \cdot 3H_2O$ (>99%, Panreac) and CH_3COOH (>99% ACS, Aldrich) were used as received.

2.2. Natural materials employed

Pumice (P) and diatomite (D) were acquired from a native supplier (Argentina, Marysol). The black sand (BS) was collected from Praia Preta (Ilha Grande, Brazil) and the natural aluminosilicate Montanit300® (M) was obtained from Montana Žalec, Slovenia. All samples were carefully washed with distilled water, dried during 48 h at room temperature and 24 h at 60ºC, and then ground into dust to **minimize** diffusional restrictions.

2.3. Characterization of the natural materials

The characterization methodology concerning the point of zero charge (pH_{PZC}), powder X-ray diffraction (XRD), emission scanning electron microscope and energy-dispersive X-ray analysis (SEM-EDX), specific surface area and pore size distribution by N_2 Physisorption and density of acid sites by temperature programmed desorption (TPD) of pyridine, were reported in previous studies by Inchaurrondo et al. (Inchaurrondo et al. 2018; Inchaurrondo et al. 2017).

2.4. Batch experiments

Adsorption tests were performed with a solid concentration of 25 g/L. The suspensions were shaken on a rotary mixer at room temperature. Aiming to test a more realistic condition, the As solutions were prepared using a bottled water matrix (Font Vella, Barcelona), which according to its label contained: 143 mg/L bicarbonates, 12.5 mg/L Na, 11.3 mg/L Mg, 42 mg/L Ca, with a conductivity of 286 µS/cm. For the sake of comparison, As(V) adsorption experiments were also performed over a ultrapure Milli-Q water matrix. The solid adsorbents

were separated by filtration (RC 0.45 μm syringe filter).

As(V) adsorption isotherms were obtained at the equilibrium pH value reached naturally for each adsorbent. The As(V) isotherms were evaluated at a concentration range between 0.5 and 6 mg/L.

The kinetic studies were performed considering different time intervals according to the above method. The initial concentration of arsenic was set at 1 mg/L and the sampling time was adjusted according to the rate of As removal for each solid sample.

To determine whether the natural adsorbents can be reused, desorption tests were performed by adding the used adsorbent (charged with As(V)) to NaOH (0.01 M) or HNO_3 (0.01 M) solutions in Milli-Q water, with a solid concentration of 25 g/L, as in the adsorption tests. Afterwards, the suspensions were shaken for 24 h and separated by filtration (RC 0.45 μm syringe filter).

The influence of **the** initial pH value on measured data was assessed in adsorption tests with 1 mg/L As solutions. The value of the starting pH was adjusted with NaOH (0.1 M) or acetate buffer (0.02 M) to regulate at pH=11 or pH=3.7, respectively.

Additionally, the influence of anion interference was studied for As(V) solutions of 1 mg/L prepared with Milli-Q water, by using an As:anion molar ratio of 1:25. The investigated anions were Cl^-, SO_4^{2-}, NO_3^- and PO_4^{3-}.

At the end of the experiments, the final pH value was registered to be reported throughout the work as **the adsorption equilibrium pH** (pH_{eq}).

2.5. Analytical measurements

Arsenic concentration was determined by Inductively Coupled Plasma Mass Spectrometry, ICP-MS (XSERIES 2 ICP-MS, Thermo Scientific, USA).

The reported values are the average of at least two measurements, and error bars represent the standard deviation.

3. Results and discussion

3.1. Characterization of adsorbents

The materials were characterized in a previous study, where the natural samples were used for catalytic purposes in the heterogeneous Fenton-like reaction (Inchaurrondo et al. 2018; Inchaurrondo et al. 2017).

Table 1 presents BET specific surface area and TPD-pyridine results for all the studied samples. Two of the materials selected, black sand and pumice, presented rather low surface areas (0.5-1 m^2/g). On the other hand, Montanit300® and diatomite showed significantly higher values, 36 and 133 m^2/g, respectively. Regarding the TPD-pyridine experiments, the adsorption of pyridine was very low, which was related to the relatively reduced BET specific surface areas observed. In the case of diatomite, its higher surface area enabled an increased hydroxyl groups exposure to pyridine and therefore, the amount of acidic sites (mmol/g) measured **was higher than the values obtained with the other samples**. Montanit300® showed a higher density of acidic sites ($mmol/m^2$) which correlates to its higher content of Al and Fe (Table 2).

The point of zero charge was similar between samples, in the case of pumice (8.7), diatomite (8.5) and Montanit300® (8.9). The black sand showed a lower value: pH_{pzc} = 7.9.

The SEM-EDX results (Table 2) showed a majority of Si, Al and Fe oxides, with minor mineral impurities, such as Ca, Ti, Na, Mn, K and Mg. Pumice, diatomite and Montanit300® samples presented a composition mostly based on SiO_2. On the other hand, the

black sand showed a composition quite different, centered in the presence of Fe and Ti oxides.

According to XRD results, pumice is primarily composed of an **abundant amorphous phase of SiO_2,** plagioclase (feldspar, which composition ranges from $NaAlSi_3O_8$ (Albite) to $CaAl_2Si_2O_8$ (Anorthite)), quartz crystals, phyllosilicates, cristobalite and calcium carbonate (Inchaurrondo et al. 2018). The black sand showed the presence of quartz, ilmenite (titanium-iron oxide mineral, weakly magnetic) and hematite (common iron oxide, Fe_2O_3) (Inchaurrondo et al. 2018). **The** Montanit300® sample exhibited the presence of natural zeolites, mainly heulandite ($Ca_{3.6}K_{0.8}Al_{8.8}Si_{27.4}O_{72}\times 26.1H_2O$) and clinoptilolite ($(Na,K,Ca)_6(Si,Al)_{36}O_{72}\times 20H_2O$), but also quartz and phyllosilicates (Inchaurrondo et al. 2018). The diffractogram of diatomite showed the presence of albite ($NaAlSi_3O_8$), nontronite (Fe(III) rich member of the smectite group in clay minerals) and quartz as main components (Inchaurrondo et al. 2017). It was also identified the amorphous silica phase (opaline silica) characteristic of diatom frustules.

3.2. Preliminary As(V) adsorption results

Preliminary As(V) adsorption studies were performed in 24-h tests, using Milli-Q water at initial pH=7.5, with As(V) concentration of 6 mg/L. These preliminary screening tests were executed in order to choose the materials with higher adsorption capacity.

Pumice showed negligible adsorption (0.0037 mg/g) under the given experimental conditions. According to the characterization results, pumice presents not only a lower surface area but also a lower content of Fe impurities, specie that promote arsenic adsorption. Pumice is mostly composed of amorphous silica; therefore, its surface is covered by inert silanol groups, which have shown low affinity towards arsenic (Shevade and Ford 2004). Consequently, pumice was not considered for further studies.

Among the materials tested, black sand showed the highest adsorption capacity (0.021 mg/g). However, unlike the other materials, its final equilibrium pH value was found to be lower than its pH_{PZC} (pH_{eq} = 7.5). The hydroxyl functional groups form on the hydrated surface of the studied minerals can protonate ($pH<pH_{PZC}$) or deprotonate ($pH>pH_{PZC}$), causing variations in the surface charge, which depends on the pH of the aqueous medium. This analysis must be correlated to the speciation state of the arsenic molecules, which also depends on solution pH. The equilibrium dissociation constants of H_3AsO_4 (As (V)) are: pKa_1=2.19, pKa_2=6.94, and pKa_3=11.5. In the case of black sand, $pH_{eq} < pH_{PZC}$ favored the adsorption of arsenic since the arsenate anion ($pH_{eq} > pKa_2$) interacted through coulombic forces with the positively charged surface.

The different adsorption capacities observed for diatomite (0.013 mg/g) and Montanit300® (0.0062 mg/g) samples could relate to the different equilibrium pH values reached: 9.9 for Montanit300® and 8.6 for diatomite. Then, Montanit300® reached equilibrium at a much more basic pH value, which is detrimental for the arsenic adsorption process.

To further compare the behavior of the materials under similar conditions, the subsequent isothermal measurements were performed at equal equilibrium pH using a more realistic water matrix elaborated with bottled water.

3.3. As(V) isotherms in a bottled water matrix

Isotherms were determined using bottled water at initial pH=8. The ions present in the water matrix buffered the pH variations caused by the addition of the solid samples. The final equilibrium pH value reached for all examined samples remained between 7.8 and 8.2. To assure equilibrium, the contact time was prolonged up to 48 h, **which agrees with the kinetic results obtained (see section 3.4). Results are presented in Fig. 1.**

The outcomes suggest that the surface area is not the governing factor for As(V) adsorption**, but** the chemical composition of the adsorbents.

Previous studies have shown that the major surface functional groups in soils and natural inorganic materials are the siloxane groups linked to the plane of oxygen atoms bound to the silica tetrahedral layer present on phyllosilicates, and the OH-groups associated with the edges of inorganic minerals such as metal oxides, oxyhydroxides, hydroxides, kaolinite and amorphous materials (Sparks 2003). Spectroscopic analyses of the crystal structures of oxides and clays showed that different types of OH-groups have different reactivity (Sparks 2003). Therefore, the composition of the samples, such as the content of amorphous SiO_2, Al or Fe clay impurities or oxides, determines the capacity and strength of adsorption.

On the subject of the removal mechanism on hydroxyl sites, arsenic adsorption may proceed through ligand exchange with OH^- and OH_2^+ functional groups, leading to complex formation. For example, partial dissociation of H_3AsO_4 releases H^+ ions which form H_2O with OH^- and leave space for arsenate binding (Siddiqui and Chaudhry 2017). Also, the complexation may proceed through either physisorption or chemisorption processes and As may attach the oxide surface via intramolecular or extra-molecular interactions (Siddiqui and Chaudhry 2017), which will be discussed later.

The highest adsorption capacity was shown by the black sand, which presented the lowest superficial area, but a composition quite different compared to diatomite and Montanit300®, which are mostly based on Si oxides. As mentioned previously, silanol surface groups show low affinity towards As (Shevade and Ford 2004). The black sand presented a high content of Fe species (mainly ilmenite and hematite) and according to several authors, iron-containing compounds present higher affinity towards arsenate compared to non-iron compounds (Youngran et al. 2007). For example, Elizalde-Gonzalez et al. (2001) related the adsorption capacity of clinoptilolite rich tuffs to the iron content of the samples. Taking into

account these characteristics and adsorption results, it can be deduced that **the** iron species present in black sand are responsible for the highest adsorption observed. However, a small quantity of red sludge was detected. Hence, co-precipitation of secondary oxides with the target metal(loid) (e.g., $FeAsO_4 \times H_2O$, $FeAsO_4 \times 2H_2O$, and $Fe_3(AsO_4)_2$) could be a key step in the removal of As using this material (Komárek et al. 2013).

Montanit300® and diatomite showed similar adsorption capacity per mass unit of adsorbent. However, if the uptake of arsenic is considered per square meter of adsorbent, Montanit300® showed a higher affinity. The lower adsorption onto diatomite could be due to the lower density of reactive hydroxyl edge sites in spite of its larger specific surface area. Montanit300® showed a higher density of acidic sites (mmol/m^2) and content of Fe and Al. The relatively high concentration of terminal Al–OH or Fe-OH species present in natural zeolites with medium/low Si/Al ratio, has been linked to its greater ability for ligand exchange; moreover, those surface groups may represent the principal reactive sites for the adsorption of As(V) (Shevade and Ford 2004).

The isotherms of the three materials fit the Freundlich model (Equation 1), which describes non-ideal and reversible adsorption.

$$q_e = K_F * C_e^{\,n} \quad (1)$$

The adsorption coefficient, K_F, is connected to the adsorption strength. The exponent n defines the isotherm curvature and the saturation speed. When $n < 1$ the isotherm shows a relative high adsorbent loading at low adsorbate concentrations, which corresponds to favorable isotherms.

According to the Freundlich model (Table 3), all materials presented favorable isotherms ($n < 1$). As expected, the black sand exhibited higher K_F, while diatomite and Montanit300® samples presented similar values. These results are directly related to the adsorption capacities observed.

Additionally, the Langmuir equation was evaluated (Equation 2). This model assumes that the adsorbent surface presents a fixed number of accessible sites with the same energy (Langmuir 1918). However, this model is not valid for heterogeneous surfaces found in soils (Sparks **2003)** and **should only be** used for qualitative comparisons.

$$q_e = \frac{Q_m * K_L * C_e}{1 + K_L * C_e} \quad (2)$$

Qm (mg/g) is defined as the maximum saturated monolayer adsorption capacity and K_L (L/mg) is related to the adsorbent/adsorbate affinity. Consequently, good adsorbents display high *Qm* and a steep initial sorption isotherm slope (high K_L).

As it was observed for the Freundlich model, the Langmuir parameters obtained for black sand were remarkably better, since it showed a higher maximum saturated monolayer adsorption capacity (*Qm)* and affinity towards the adsorbate (K_L) (Table 3). Diatomite and Montanit300® presented similar parameters. As described previously, if the parameters are considered per square meter of adsorbent (Q'_{max}), Montanit300® showed higher affinity towards As(V) compared to diatomite, which is related to its higher density of acidic sites (mmol/m^2) and content of Fe and Al.

The maximum saturated monolayer adsorption capacity values observed in this study (Q_{max}=0.065-0.033 mg/g) are in agreement with some of the results obtained with other materials of natural origin and used without any pretreatment, **such as presented in Table 4. The higher adsorption values observed for some of these natural materials are related to their amorphous nature (higher surface area and density of hydroxyl sites) and higher aluminum and/or iron content. In addition, water matrix and pH may differ between tests. Since the adsorption capacities are much lower for unmodified natural materials, a greater amount of adsorbent may be required to achieve the recommended arsenic levels. Then, these materials are suited for systems with relatively low As concentrations (µg/L levels) such as leachates from altered rocks (Tabelin et al. 2014). Moreover, the**

higher adsorbent load requirement can be compensated by the lower cost of these raw materials and the avoidance of the environmental impact (CO_2 emission) related to the modification or synthesis of more sophisticated materials.

3.4. As(V) kinetics curves

Previous studies have reported the existence of a wide time scale for soil chemical reactions, which ranges from microseconds to years (Sparks 2003). Ion association (ion pairing, complexation, and chelation-type reactions in solution), ion exchange and some sorption reactions may take **remarkable short times**, ranging from microseconds **to** milliseconds. On the other hand, mineral solution (precipitation/dissolution reactions including discrete mineral phases) and mineral crystallization reactions can take years. Moreover, these reactions can occur simultaneously and consecutively (Sparks 2003). Considering this, kinetic studies were performed to study the feasibility of implementing the proposed materials in adsorption processes, hopping to obtain short reaction times. Tests were executed with As(V) concentration of 1 mg/L in a bottled water matrix. The obtained results are presented in Fig. 2.

The adsorption of arsenic was practically instantaneous in the case of Montanit300®. **A fast solute removal** as well as a low equilibration time are connected to highly favorable sorptive interactions. The faster uptake could be connected to a higher surface area, in contrast to the black sand and also a higher density of acidic sites (mmol/m^2), in comparison to diatomite. Furthermore, Montanit300® presents a higher content of Fe and Al. As mentioned before, a higher concentration of terminal Al–OH species in low Si/Al ratio zeolites enhances ligand exchange reactions (Shevade and Ford 2004). Another likely mechanism for the removal of anions in zeolites could involve the interaction with

extraframework cations (such as Na^+, Ca^{2+} or Mg^{2+}), forming the corresponding salt in the voids of the zeolite (Uzunova and Mikosch 2016).

As it can be seen in Fig.2-b, diatomite reaches equilibrium after only one hour, probably due to its high surface area and pore volume. The black sand reaches equilibrium after approximately 24 h. In spite of showing a high content of Fe species, its surface area is very low.

After the first hour, diatomite, Montanit300® and black sand showed similar adsorption values of 0.005, 0.006 and 0.005 mg/g, respectively. After two days, black sand reached a final equilibrium value of 0.016 mg/g (2.7 times higher).

To evaluate the sorption rates, empirical pseudo-first (Equation 3) and pseudo-second order (Equation 4) equations were adopted to model the experimental data (Table 3).

$$\frac{dq_t}{dt} = k_1 * (q_e - q_t) \quad (3)$$

$$\frac{dq_t}{dt} = k_2 * (q_e - q_t)^2 \quad (4)$$

The constants k_1 (1/min) and k_2 (g/(mg min)) are the pseudo-first order and the pseudo-second order rate constants, respectively, while q_t and q_e are the arsenic adsorption amounts (expressed in mg/g) at any time (t (min)) and at equilibrium, respectively.

Since adsorption was instantaneous in the case of Montanit300®, the results did not fit any of the two models. Black sand and diatomite fit reasonably both models (Table 3). The kinetic constant obtained for black sand is quite low and even though the adsorption capacity is higher, a slow kinetic is an unfavorable characteristic for an appropriate adsorbent material. The red sludge observed could be associated to the slower kinetics shown by the formation of surface precipitates (Sparks 2003).

In the case of Montanit300®, the uptake of arsenic was instantaneous (seconds or miliseconds). Similar studied materials such as natural or modified zeolites, presented much larger equilibration times, from minutes to hours or days (Bilici Baskan and Pala 2011;

Elizalde-González et al. 2001; Jiménez-Cedillo et al. 2009; Shevade and Ford 2004; Šiljeg et al. 2012).

3.5. pH effect in As(V) adsorption

The pH effect was addressed in order to understand the nature of the arsenic-adsorbent interactions. The adsorption capacity and final equilibrium pH are presented in Figs.3 a)-b). According to these results, in the case of diatomite, the adsorption capacity is less influenced by pH changes, since a relative variation of only 16% was measured for adsorption levels at different pH values. Arsenic removal may not be strongly related to electrostatic interactions in this case. Black sand and Montanit300® showed higher adsorption levels under acidic pH. Low pH values generate the protonation of surface hydroxyl groups to $-OH_2^+$, which facilitates the ligand exchange since H_2O is easier to displace from metal binding sites than OH^- (García- Sanchez et al. 2002). This effect was more notorious in the case of black sand, which also sustains significant levels of adsorption even under neutral or slightly basic pH conditions (7.5-8.0), which is a common value in underground and surface water resources. The fact that there is still some adsorption when the pH value is higher than pH_{PZC}, can be attributed to a specific inner sphere bonding of arsenate to the surface of the solid.

The adsorption capacity drastically drops at pH values higher than 8 in the case of Montanit300®. The pH dependency indicates a strong electrostatic attraction mechanism, which means that arsenic oxyanions are mostly adsorbed non-specifically by strong electrostatic interactions.

3.6. Anions interference

The influence of different anions in the adsorption of As(V) using a Milli-Q water matrix is shown in Fig. 4. It is important to highlight that different equilibrium pH values were reached

at the end of the tests for each material: 9.7 for Montanit300®, 7.4 for black sand and 8.6 for diatomite.

Phosphate and arsenate present similar structure (charge and same tetrahedral configuration) and compete for binding sites (Youngran et al. 2007), which explains the 90 % removal reduction registered for all the materials tested with ultrapure water spiked with phosphate.

Under the employed operating conditions, the addition of the other anions, NO_3^-, SO_4^{2-} and Cl^- did not cause a significant variation on As(V) adsorption in comparison to PO_4^{3-}. Relative variabilities of 14, 12 and 6%, were registered regarding arsenic removal in Milli-Q water or NO_3^-, SO_4^{2-} and Cl^- containing solutions, for Montanit300®, diatomite and black sand, respectively. Other authors observed similar results, although this observation depends on both concentration and pH values. The complexes formed with these anions (nitrate, sulphate and chloride) resulted much weaker than those formed with arsenate (Youngran et al. 2007).

3.7. Desorption tests

Desorption tests using HNO_3 and NaOH (Table 5), showed that the black sand is difficult to regenerate (only 17 to 49 % recovered). The arsenic that was not leached was probably either strongly adsorbed (inner sphere complex) or co-precipitated with iron oxide species. The adsorption through inner-sphere complexation is not greatly influenced by the alteration of solution ionic strength, compared to outer-sphere complexation (Hua 2018). However, the pH dependency observed before indicates a strong electrostatic attraction mechanism step. Consequently, it is possible that the arsenic oxyanions are predominantly adsorbed non-specifically by a strong electrostatic interaction, followed by inner-sphere complexation between arsenic oxyanions and OH-groups on the surface of the adsorbent (Hua 2018).

Diatomite showed a high and equal level of As desorption under acidic or basic pH. This is very well related to the observed insensitivity of the material towards pH changes. The arsenic sorption through weak physical interactions may be the main mechanism responsible of this behavior.

In the case of Montanit300®, arsenic was totally desorbed under alkaline conditions. As it was observed in tests where the pH effect was assessed, arsenic adsorption was highly inhibited under basic pH values. Therefore, this behavior can be explained by taking into consideration the electrostatic interaction and ion exchange mechanism that may prevail in the case of this material.

4. Conclusions

Four different iron-bearing geo-adsorbents were selected to be tested for As(V) removal without any pretreatment: Montanit300® (M), diatomite (D), pumice (P) and black sand (BS), in order to choose the best one in terms of adsorption capacity, kinetics, regeneration capability and stability. The premise of the study was to select an adsorbent among cheap and available materials with characteristics that are functional to the arsenic removal process: high surface area and/or the presence of iron species in their composition.

The following conclusions were drawn:

- **Surface area was not the dominating factor for adsorption capacity, but the chemical composition of the adsorbents.**
- **P exhibited negligible adsorption due to its lower content of Fe or Al impurities and surface area.**

- **BS presented a low surface area, but the highest content of Fe species, which resulted in the highest adsorption capacity (0.045 mg/L) with a slow kinetic (24 h).**
- **M and D presented similar adsorption capacities (0.02 mg/g).**
- **M showed the fastest solute removal (seconds), which was related to its higher density of acidic sites (mmol/m^2).**
- **Only phosphate ions showed a negative effect on As adsorption.**
- **The pH effect was only relevant for BS and M (adsorption increased under acidic pH).**
- **Desorption was properly achieved for D (80-85 %) and M (100 %) samples, but not for BS (50%), by using NaOH.**
- **M showed the most promising features: remarkably fast adsorption kinetic and easy regeneration.**
- **The materials are suited for systems with relatively low As concentrations (µg/L levels) such as leachates from altered rocks.**

Acknowledgements - This work was supported by CONICET, UNMdP, Marie Skłodowska-Curie Actions: Research and Innovation Staff Exchange (RISE) under the title "Advanced multifunctional materials applied to remove arsenic in Argentinian groundwater" (NANOREMOVAS project n.645024). We also want to express our gratitude to Dr. P. Caracciolo for his technical support.

References

- Ahmaruzzaman, M., Gupta, V.K., 2011. Rice husk and its ash as low-cost adsorbents in water and wastewater treatment. Ind. Eng. Chem. Res. 50, 13589–13613. dx.doi.org/10.1021/ie201477c.

- Asere, T.G., Stevens, C.V., Laing, G.D., 2019. Use of (modified) natural adsorbents for arsenic remediation: A review. Science of The Total Environment. 676, 706-720. https://doi.org/10.1016/j.scitotenv.2019.04.237.
- Bajpai, S., Chaudhuri, M., 1999. Removal of Arsenic from Ground Water by Manganese Dioxide–Coated Sand. Journal of Environmental Engineering. 125, 782–784. https://doi.org/10.1061/(ASCE)0733-9372(1999)125:8(782).
- Bentahar, Y., Hurel, C., Draoui, K., Khairoun, S., Marmier, N., 2016. Adsorptive properties of Moroccan clays for the removal of arsenic (V) from aqueous solution. Applied Clay Science 119, 385–392. https://doi.org/10.1016/j.clay.2015.11.008.
- Bilici Baskan, M., Pala, A., 2011. Removal of arsenic from drinking water using modified natural zeolite. Desalination. 281, 396–403 https://doi.org/10.1016/j.desal.2011.08.015.
- Boglione, R., Griffa, K., Panigatti, M.C., Keller, S., Schierano, M.C., Asforno, M., 2019. Arsenic adsorption by soil from Misiones province, Argentina. Environ. Technol. Innov.13, 30-36. https://doi.org/10.1016/j.eti.2018.10.002.
- Burakov, A.E., Galunin, E.V., Burakova, I.V., Kucherova, A.E., Agarwal, S., Tkachev, A.G., Gupta, V.K., 2018. Review: Adsorption of heavy metals on conventional and nanostructured materials for wastewater treatment purposes: A review. Ecotoxicology and Environmental Safety. 148, 702–712. https://doi.org/10.1016/j.ecoenv.2017.11.034.
- Çifçi, D.İ., Meriç, S., 2016. A review on pumice for water and wastewater treatment. Desalination and Water Treatment. 57, 18131–18143. https://doi.org/10.1080/19443994.2015.1124348.
- Danil de Namor, A.F., El Gamouz, A., Frangie, S., Martinez, V., Valiente, L., Webb, O.A., 2012. Turning the volume down on heavy metals using tuned diatomite. A review of diatomite and modified diatomite for the extraction of heavy metals from water. Journal of Hazardous Materials. 241–242, 14–31. https://doi.org/10.1016/j.jhazmat.2012.09.030.
- Elizalde-González, M.P., Mattusch J., Wennrich R., Morgenstern P., C., 2001. Uptake of arsenite and arsenate by clinoptilolite-rich tuffs. Microporous and Mesoporous Materials. 46, 277–286. https://doi.org/10.1016/S1387-1811(01)00308-0.
- García- Sanchez, A., Alvarez-Ayuso, E., Rodriguez-Martin, F., 2002. Sorption of As(V) by some oxyhydroxides and clay minerals. Application to its immobilization in two polluted mining soils. Clay Minerals. 37, 187–194. https://doi.org/10.1180/0009855023710027.
- Ghosh, D., Gupta, A., 2012. Economic justification and eco-friendly approach for regeneration of spent activated alumina for arsenic contaminated groundwater treatment. Resources, Conservation and Recycling. 61, 118-124. https://doi.org/10.1016/j.resconrec.2012.01.005.
- Gu, H., Xu, X., Zhang, H., Liang, C., Lou, H., Ma, C., Li, Y., Guo, Z., Gu, J., 2018. Chitosan-coated-magnetite with covalently grafted polystyrene based carbon nanocomposites for hexavalent chromium adsorption. Eng. Sci. 1, 46–54. doi: 10.30919/espub.es.180308.
- Gupta, V.K., Nayak, A., Agarwal, S., 2015. Bioadsorbents for remediation of heavy metals: Current status and their future prospects. Environ. Eng. Res. 20(1): 1-18. http://dx.doi.org/10.4491/eer.2015.018.
- Gupta, V. K., Suhas, Tyagi, I., Agarwal, S., Singh, R., Chaudhary, M., Harit, A., Kushwaha, S., 2016. Column operation studies for the removal of dyes and phenols using a low cost adsorbent. Global J. Environ. Sci. Manage., 2(1): 1-10. https://doi.org/10.7508/gjesm.2016.01.001.
- Hua, J., 2018. Adsorption of low-concentration arsenic from water by co-modified bentonite with manganese oxides and poly(dimethyldiallylammonium chloride). Journal of Environmental Chemical Engineering. 6, 156–168. https://doi.org/10.1016/j.jece.2017.11.062.
- Inchaurrondo, N., Maestre, A., Žerjav, G., Pintar, A., Ramos, C., Haure, P., 2018. Screening of catalytic activity of natural iron-bearing materials towards the Catalytic Wet Peroxide Oxidation of Orange II. Journal of Environmental Chemical Engineering. 6, 2027–2040. https://doi.org/10.1016/j.jece.2018.03.001.

- Inchaurrondo, N., Ramos, C.P., Žerjav, G., Font, J., Pintar, A., Haure, P., 2017. Modified diatomites for Fenton-like oxidation of phenol. Microporous and Mesoporous Materials. 239, 396–408. https://doi.org/10.1016/j.micromeso.2016.10.026.
- Jiménez-Cedillo, M.J., Olguín, M.T., Fall, Ch., 2009. Adsorption kinetic of arsenates as water pollutant on iron, manganese and iron–manganese-modified clinoptilolite-rich tuffs. Journal of Hazardous Materials. 163, 939–945. https://doi.org/10.1016/j.jhazmat.2008.07.049.
- Kalaruban, M., Loganathan, P., Nguyen,T.V., Nur, T., Johir, M.A.H., Nguyen, T.H.,Trinh, M.V., Vigneswaran, S., 2019. Iron-impregnated granular activated carbon for arsenic removal: Application to practical column filters. Journal of Environmental Management 239, 235-243. https://doi.org/10.1016/j.jenvman.2019.03.053.
- Komárek, M., Vaněk, A., Ettler, V., 2013. Chemical stabilization of metals and arsenic in contaminated soils using oxides – A review. Environmental Pollution. 172, 9–22. https://doi.org/10.1016/j.envpol.2012.07.045.
- Langmuir, I., 1918. The adsorption of gases on plane surfaces of glass, mica and platinum. Journal of the American Chemical Society. 40, 1361–1403. https://doi.org/10.1021/ja02242a004.
- Litter, M.I., Morgada, M.E., Bundschuh, J., 2010. Possible treatments for arsenic removal in Latin American waters for human consumption. Environmental Pollution. 158, 1105–1118. https://doi.org/10.1016/j.envpol.2010.01.028.
- Liu, B., Liu, Z., Wu, H., Pan, S., Cheng, X., Sun, Y., Xu, Y., 2020. Effective and simultaneous removal of organic/inorganic arsenic using polymer-based hydrated iron oxide adsorbent: Capacity evaluation and mechanism. Science of The Total Environment. 742, 140508. https://doi.org/10.1016/j.scitotenv.2020.140508.
- Maji, S.K., Pal, A., Pal, T., 2007. Arsenic removal from aqueous solutions by adsorption on laterite soil. Journal of Environmental Science and Health, Part A. 42, 453–462. https://doi.org/10.1080/10934520601187658.
- Manning, B.A., 1996. Modeling Arsenate Competitive Adsorption on Kaolinite, Montmorillonite and Illite. Clays and Clay Minerals. 44, 609–623. https://doi.org/10.1346/CCMN.1996.0440504.
- Mar, K.K., Karnawati, D., Sarto, Putra, D.P.E., Igarashi, T., Tabelin, C.B., 2013. Comparison of Arsenic Adsorption on Lignite, Bentonite, Shale, and Iron Sand from Indonesia. Procedia Earth and Planetary Science. 6, 242–250 . https://doi.org/10.1016/j.proeps.2013.01.033.
- Palma-Lara, I., Martínez-Castillo, M., Quintana-Pérez, J.C., Arellano-Mendoza, M.G., Tamay-Cach, F., Valenzuela-Limón, O.L., García-Montalvo, E.A., Hernández-Zavala, A., 2020. Arsenic exposure: A public health problem leading to several cancers. Regulatory Toxicology and Pharmacology. 110, 104539. https://doi.org/10.1016/j.yrtph.2019.104539.
- Shevade, S., Ford, R.G., 2004. Use of synthetic zeolites for arsenate removal from pollutant water. Water Research. 38, 3197–3204. https://doi.org/10.1016/j.watres.2004.04.026.
- Siddiqui, S.I., Chaudhry, S.A., 2017. Iron oxide and its modified forms as an adsorbent for arsenic removal: A comprehensive recent advancement. Process Safety and Environmental Protection. 111, 592–626. https://doi.org/10.1016/j.psep.2017.08.009.
- Šiljeg, M., Foglar, L., Gudelj, I., 2012. The removal of arsenic from water with natural and modified clinoptilolite. Chemistry and Ecology. 28, 75–87. https://doi.org/10.1080/02757540.2011.619531.
- Singh, E., Kumar, A., Khapre, A., Saikia, P., Kumar Shukla, S., Kumar, S., 2020. Efficient removal of arsenic using plastic waste char: Prevailing mechanism and sorption performance. Journal of Water Process Engineering. 33, 101095.https://doi.org/10.1016/j.jwpe.2019.101095.
- Smedley, P.L., Kinniburgh, D.G., 2002. A review of the source, behaviour and distribution of arsenic in natural waters. Applied Geochemistry. 17, 517–568. https://doi.org/10.1016/S0883-2927(02)00018-5.
- Sparks, D. L., 2003 'Environmental Soil Chemistry', 2nd. Ed. Elsevier-Academic Press, New York.

- Suhas, Gupta, V.K., Carrott, P.J.M., Singh, R., Chaudhary, M., Kushwaha, S., 2016. Review Cellulose: A review as natural, modified and activated carbon adsorbent. Bioresource Technology. 216, 1066–1076. http://dx.doi.org/10.1016/j.biortech.2016.05.106.
- Tabelin, C.B., Igarashi, T., Arima, T., Sato, D., Tatsuhara, T., Tamoto, S., 2014. Characterization and evaluation of arsenic and boron adsorption onto natural geologic materials, and their application in the disposal of excavated altered rock. Geoderma 213, 163–172. https://doi.org/10.1016/j.geoderma.2013.07.037.
- Thirunavukkarasu, O. S., Viraraghavan, T. and Subramanian, K. S., 2003. Arsenic Removal from Drinking Water using Iron Oxide-Coated Sand. Water, Air, & Soil Pollution. 142, 95–111. https://doi.org/10.1023/A:1022073721853.
- Uzunova, E.L., Mikosch, H., 2016. Adsorption of phosphates and phosphoric acid in zeolite clinoptilolite: Electronic structure study. Microporous and Mesoporous Materials. 232, 119–125. https://doi.org/10.1016/j.micromeso.2016.06.019.
- Wang, B., Wu, T., Angaiah, S., Murugadoss, V., Ryu, J-E., Wujcik, E.K., Lu, N., Young, D.P., Gao, Q., Guo, Z., 2018. Development of nanocomposite adsorbents for heavy metal removal from wastewater. ES Mater. Manuf. 2, 35‑44. doi: 10.30919/esmm5f175.
- Wei, H., Ma, J., Shi, Y., Cui, D., Liu, M., Lu, N., Wang, N., Wu, T., Wujcik, E.K., Guo, Z., 2018. Sustainable cross-linked porous corn starch adsorbents with high methyl violet adsorption. ES Mater. Manuf. 2, 28‑34. doi: 10.30919/esmm5f162.
- World Health Organization. Arsenic in Drinking-water. Background document for development of WHO Guidelines for Drinking-water Quality (2011).
- Youngran, J., Fan, M., Van Leeuwen, J., Belczyk, J.F., 2007. Effect of competing solutes on arsenic(V) adsorption using iron and aluminum oxides. Journal of Environmental Sciences. 19, 910–919. https://doi.org/10.1016/S1001-0742(07)60151-X.
- Zehhaf, A., Benyoucef, A., Quijada, C., Taleb, S., Morallón, E., 2015. Algerian natural montmorillonites for arsenic(III) removal in aqueous solution. International Journal of Environmental Science and Technology. 12, 595–602. https://doi.org/10.1007/s13762-013-0437-3.
- Zhao, J., Boada, R., Cibin, G., Palet, C., 2020. Enhancement of selective adsorption of Cr species via modification of pine biomass. Science of the Total Environment. 143816. https://doi.org/10.1016/j.scitotenv.2020.143816.

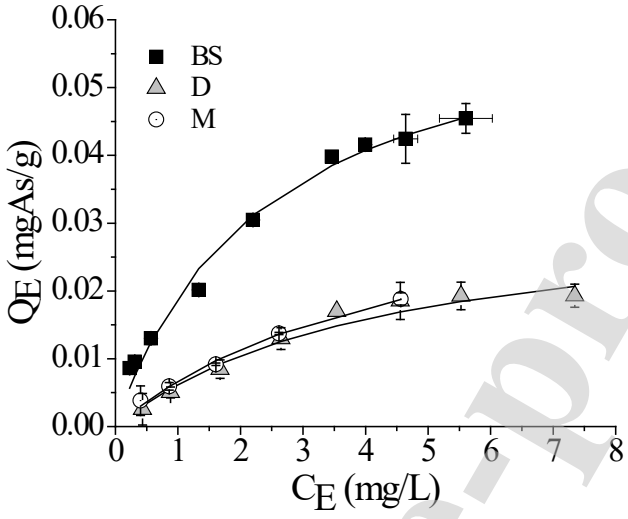

Fig. 1 As(V) adsorption isotherms determined at 25°C after 48 h in bottled water matrix with initial pH=8. Lines correspond to the Langmuir model. Error bars indicate the standard deviation of the experiments.

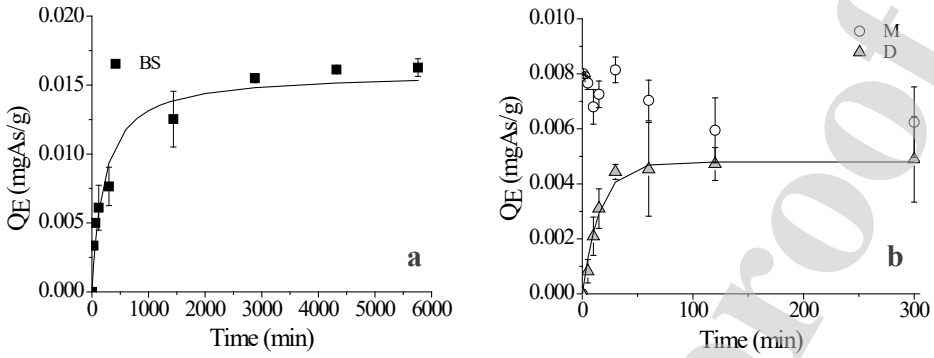

Fig. 2 As(V) adsorption in bottled water matrix, kinetic curves (C_0=1 mg/L, 25ºC, pH_0=8): a) Black sand, b) Diatomite and Montanit300®. The kinetic curves correspond to the pseudo-first order model in the case of Black sand, and pseudo-second order model in the case of Diatomite. Error bars indicate the standard deviation of the experiments.

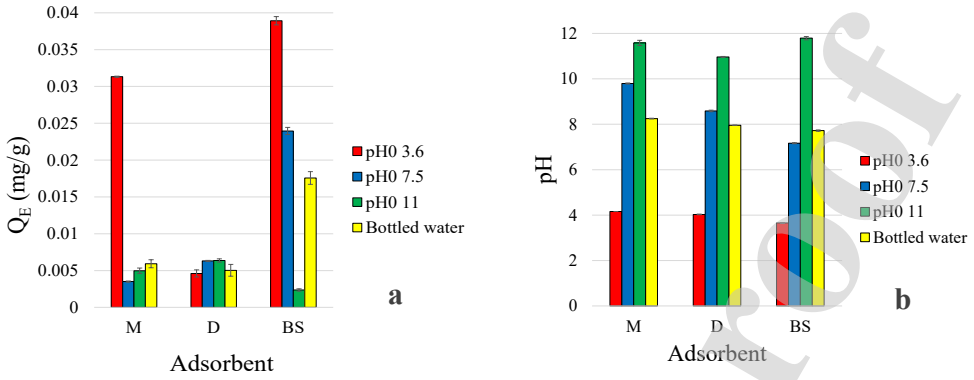

Fig. 3 a) Adsorption capacity and b) final equilibrium pH of investigated adsorbents for As(V) removal. Experimental conditions: C_0=1 mg/L, 25 g/L of adsorbent, measurements carried out after 24 h (M and D) and 48 h (BS). Matrix: 0.02 M acetate buffer at pH_0=3.7, Milli-Q water at pH_0=7.5, 0.01 M NaOH solution at pH_0=11.5, and bottled water at pH_0=8. Error bars indicate the standard deviation of the experiments.

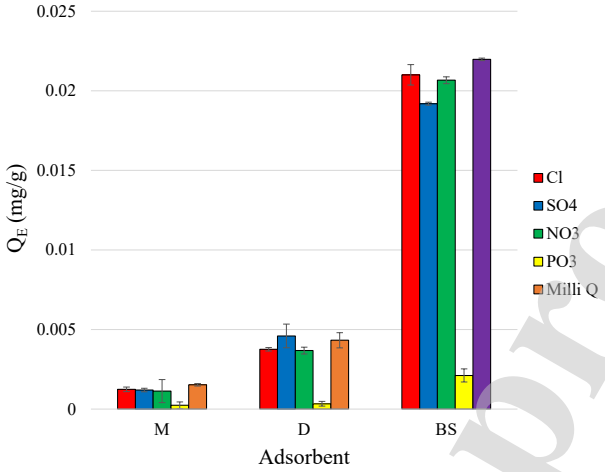

Fig. 4 Anions interference effect on As(V) adsorption capacity. Experimental conditions: [As(V)]:[anion]$_{mol}$=1:25, T=25ºC, measurements were conducted after 24 h (M and D) and 48 h (BS). Error bars indicate the standard deviation of the experiments.

Table

Table 1. Results of N_2 physisorption, surface acidity and pH_{PZC} measurements for samples investigated in this study (Inchaurrondo et al. 2017, 2018).

Sample	S_{BET}	V_{pore}	Density of acid sites	Quantity of acid sites	T of desorption of pyridine	pH_{PZC}
	m^2/g	cm^3/g	$mmol/m^2$	mmol/g	°C	
Black sand	0.6	0.002	0.0011	7.2×10^{-4}	240, 290, 376	7.9
Diatomite	133	0.29	0.0013	0.18	209	8.5
Pumice	1.2	0.003	0.0013	9.8×10^{-4}	170, 245, 340	8.7
Montanit300®	36	0.07	0.0038	0.14	259	8.9

Table 2. Results of SEM-EDX analysis of investigated samples (Inchaurrondo et al. 2017, 2018).

Sample	SEM-EDX composition, wt.%										
	O	Al	Si	Ti	Mn	Fe	Ca	Na	Mg	K	C
Black sand	26.8	2.0	1.82	28.2	2.1	39	-	-	-	-	-
Diatomite	39.2	4.7	33.0	-	-	3.0	0.23	0.2	1.6	-	18
Pumice	56.5	5.3	29.6	-	-	1.0	2.0	2.0	0.70	2.5	-
Montanit300®	51.8	6.7	29.6	-	-	5.9	1.8	1.0	1.4	1.8	-

Table 3. Freundlich and Langmuir isotherm parameters and kinetics constants.

Adsorbent	pH_{eq}	Adsorption isotherms								Adsorption kinetics			
		Freundlich				Langmuir				Pseudo-first order		Pseudo-second order	
		R^2	n	K_F	K'_F	R^2	Q_{max}	Q'_{max}	K_L	k_1	R^2	k_2	R^2
				$mg^{n-1} \times L^n/g$	$mg^{n-1} \times L^n/m^2$		mg/g	mg/m^2	L/mg	1/min		g/(mg min)	
Black sand	8.01	0.99	0.54	0.019	0.032	0.99	0.065	0.11	0.42	0.0030	0.93	0.30	0.96
Diatomite	7.91	0.92	0.59	0.0067	0.00005	0.97	0.033	0.00025	0.24	0.063	0.98	12	0.95
Montanit300®	8.19	0.99	0.67	0.0069	0.00019	0.99	0.038	0.0011	0.22	-	-	-	-

Table 4. Langmuir maximum saturated monolayer adsorption capacity reported in literature using different geo-adsorbents.

Natural geo-adsorbent	pH	T	As(V) Langmuir adsorption capacity	Equilibrium time	Ref.
		ºC	mg/g		
Zeolite rich rocks	4	23	0.006-0.1	7 days	Elizalde Gonzales et al. 2001
Iron sand	6.7-6.8	Room T	0.024	24-48 h	Mar el at. 2007
Laterite soil	5.7	25	0.04	4 h	Maji et al. 2007
Croatian and Serbian Na-zeolite		25	0.036-0.07	3 h	Šiljeg et al. 2012
Diatomite	8	Room T	0.033	1 h	This study
Montanit300®	8	Room T	0.038	Seconds	This study
Black sand	8	Room T	0.065	24 h	This study
Shale	7.5-7.8	Room T	0.138	24-48 h	Mar et al. 2007
Pumiceous tuffs, volcanic ashes, marine sediments	6	Room T	0.287-3.15	24 h	Tabelin et al. 2014
Bentonite	6.5-7	Room T	0.334	24-48 h	Mar et al. 2007
Moroccan clays	7	Room T	0.561-1.076	4-10 days	Bentahar et al. 2016
Lateritic soil	7	25	2	24 h	Boglione et al. 2018

Table 5. Arsenic desorption percentage by using HNO_3 and NaOH (0.01 mol/L); 24 h, 25ºC, 25 g/L of adsorbent.

	Desorption (%)		
	Black sand	Montanit300®	Diatomite
HNO_3	17.5±1.3	37.6±2.4	85.0±4.7
NaOH	48.9±1.2	100±1	80.8±3.3

Highlights

- Chemical composition and not surface area was the dominating factor for adsorption
- Fe or Al clay impurities promote arsenic adsorption
- Black sand showed the highest adsorption capacity
- Montanit300® showed better regeneration capability and remarkably fast kinetics
- Adsorption involves surface complexation and electrostatic interaction

Authors contribution statement

Inchaurrondo N.: Conceptualization, methodology, investigation, validation, writing original draft, funding acquisition.

di Luca C.: Methodology, investigation, reviewing and editing.

Haure P.: Reviewing.

Žerjav G.: Methodology, investigation, reviewing and editing.

Pintar A.: Resources, reviewing and editing.

Palet C.: Supervision, resources, reviewing and editing, funding acquisition.

*Corresponding author. *E-mail address:* ninchaurrondo@gmail.com.

Declaration of interests

☒ The authors declare that they have no known competing financial interests or personal relationships that could have appeared to influence the work reported in this paper.

☐The authors declare the following financial interests/personal relationships which may be considered as potential competing interests: